ISSN 1028-334X, Doklady Earth Sciences, 2007, Vol. 417A, No. 9, pp. 1386–1392. © Pleiades Publishing, Ltd., 2007.
Original Russian Text © V.G. Sakhno, 2007, published in Doklady Akademii Nauk, 2007, Vol. 417, No. 4, pp. 528–534.

GEOCHEMISTRY

Isotopic–Geochemical Characteristics and Deep-Seated Sources of the Alkali Rocks of the Pektusan Volcano

Corresponding Member of the RAS V. G. Sakhno

Received June 27, 2007

DOI: 10.1134/S1028334X07090206

Late Cenozoic volcanic rocks are widespread in the Russian Far East. They are mainly represented by eruptions of basaltic lavas, which compose the Sovgavan, Nelminskii, Shufanskii, and Shkotovskii plateaus, among others. Alkali basalts with xenoliths of spinel lherzolites compose monogenetic volcanoes and their vents along the deep-seated Tan Lu fault system in Northeast China and in the Ussuri–Amur rift system of the Primor'e and Amur regions, as well as along the faults of the Tokin Stanovik. Some volcanoes (Bolonski, Udalyanchi, Keluo, and others) consist of potassic alkali basaltoids (leucitic basanites, leucitites, trachybasalts, and other rocks) [1, 2, and others].

Alkali basalt–trachyte volcanoes and their flows are rare. Only two centers, the plateau in the Bikin River basin (Primorye) and the Pektusan Volcano, are known in the Far East. The first object is a zone of areal volcanism with numerous extrusions and vents of Late Miocene alkali basalts and extrusive trachyte covers [1], which overlie the volcanosedimentary complexes of the Sikhote Alin fold system. The second object, Pektusan stratovolcano, is a center of modern volcanism in the continental part of the Far East. The explosive activity of this volcano was manifested as repeated catastrophic explosions in the Pleistocene and Holocene. The most powerful explosions approximately 1 ka ago (969 ± 20) ejected a large amount of tephra (about 100 km^3) and gases (Cl, F, and vapors of S and H_2O) [3]. The explosion was directed to the east, and ashes reached the Japanese islands [4] and, partially, the southern Primor'e region of Russia.

The Pektusan Volcano (42°06′ N, 128°04′ E) consists of lava–pyroclastic (trachyte–comendite–rhyolite) rocks, which are crosscut by vents and dikes of alkali basalts, trachybasalts, and trachyandesites. The cone is located on the alkali basalts of the shield volcano. The detailed structure and composition of rocks of the volcano are reported in [5–7 and others].

New data on the isotopic dating of volcanic complexes [7] made it possible to determine time intervals of the volcano formation and to distinguish cycles of the most intense explosions (including catastrophic ones) and elucidate the evolution of magmas. Based on the $^{143}Nd/^{144}Nd$ and $^{87}Sr/^{86}Sr$ isotopic characteristics and trace element distribution, we determined deep-seated sources, their isotopic heterogeneity, and criteria of explosibility of alkali salic melts.

The oldest rocks among the basaltoids of the shield volcano are represented by the 2.34-Ma-old alkali olivine–pyroxene basalts, which compose the lower parts of the covers (Table 1). The younger volcanics with an age of 1.70 and 1.41 Ma are high-Fe Ti-alkali basalts with elevated contents of radiogenic Sr (0.705230–0.705374) and a narrow range of the $^{143}Nd/^{144}Nd$ ratio (0.512605–0.512692). The overlying subalkaline basalts with an age of 1.01–1.20 Ma are characterized by lower contents of Ti, Fe, and alkalis; lower Sr isotopic ratios (0.704452–0.704550); and narrow variations of Nd isotopic ratios. The next group of alkali basalts (from 330 to 245 and 240 ka old) comprises sills, dikes, and vents, which intrude rocks of the trachytic cone of the volcano. The latter rocks are enriched in radiogenic Sr relative to subalkaline basalts, but depleted in radiogenic Sr relative to high-Ti alkali basalts of the lower and middle parts of the shield volcano (0.704770–0.704910). The $^{143}Nd/^{144}Nd$ ratio is within the range of values typical for basalts of the shield volcano (0.512605–0.512682). Trachybasaltic pipes with an age of 100–125 ka are observed on the northern and western slopes of the volcano. In terms of the $^{87}Sr/^{86}Sr$ composition, they are similar to the subalkaline basalts of the shield volcano, but significantly depleted in the $^{143}Nd/^{144}Nd$ ratio.

The data presented above demonstrate the heterogeneity of isotopic sources, especially with respect to the radiogenic Sr. The Sr–Nd isotopic diagram shows three

Far East Geological Institute, Far East Division, Russian Academy of Sciences, pr. Stoletiya Vladivostoka 159, Vladivostok, 660022 Russia; e-mail: sakhno@fegi.ru

Table 1. Isotope data on the Pektusan Volcano

Stage	Cycle	Rock, facies	Samples	Age: K–Ar (Ma) [7]; ^{14}C (ka, years)	$^{87}Sr/^{86}Sr$	$^{143}Nd/^{144}Nd$
Post-caldera	II	Rhyolite pumice	4	1903	0.705579 ± 12	0.512583 ± 5
		Comendite pumice	26/1a	1903	0.704960 ± 13	0.512598 ± 5
		Black trachyte pumice from comendite	26/1b	1903	0.705160 ± 11	0.512608 ± 6
	I	Trachyte ignimbrite	3a	1702	0.705300 ± 12	0.512662 ± 10
		Trachyte ignimbrite	38/4	1702	0.705416 ± 10	0.512595 ± 6
Caldera	IV	Pantellerite tuff, ignimbrite	1d	969 ± 20 AD*	0.705854 ± 12	0.512610 ± 3
		Scoria, fragments, and ashes of comendite and pantellerite	1b	969 ± 20 AD*	0.705678 ± 6	0.512630 ± 6
	III	Trachyte ashes	28/4b	>2000 BP	0.705270 ± 22	0.512637 ± 8
	II	Tephra and fragments of trachyte	29/3c	0.040–0.065 ± 0.03	0.704639 ± 7	0.512617 ± 8
		Trachyte pumice from breccia	1 i	0.065 ± 0.015	0.705470 ± 22	0.512611 ± 11
		Trachyte, ignimbrite flow	26/16	0.065 ± 0.015	0.705772 ± 16	0.512635 ± 7
		Trachyte, ignimbrite flow	26/12	0.095 ± 0.015	0.704285 ± 12	0.512552 ± 8
	I	Trachybasalt, pipe	28/1	0.100–0.125 ± 0.025	0.704351 ± 11	0.512597 ± 6
Formation of volcanic cone	III	Trachytic cover	20	0.135 ± 0.025	0.704898 ± 17	0.512607 ± 4
		Trachyte ignimbrite	38/3	0.140 ± 0.015	0.705348 ± 10	0.512621 ± 6
	II	Pipe of alkali basalts	21/1	0.245 ± 0.03	0.704830 ± 13	0.512642 ± 11
		The same	28/19a	0.245 ± 0.03	0.704720 ± 10	0.512682 ± 7
		»	28/20b	0.240 ± 0.03	0.704910 ± 11	0.512638 ± 9
		Alkali basaltic sill	40/3	0.330 ± 0.050	0.704870 ± 11	0.512605 ± 6
	I	Trachytic cover	30	0.545 ± 0.05	0.705630 ± 20	0.512597 ± 7
Shield volcano	III	Trachytic cover	14/1	1.00 ± 0.05	0.705130 ± 15	0.512646 ± 11
	II		32	1.01 ± 0.2	0.704550 ± 15	0.512668 ± 8
		Subalkaline basalt, cover	23/2	1.20 ± 0.25	0.704452 ± 22	0.512686 ± 11
	I	Fe–Ti alkali basalt, cover	27/7	1.41 ± 0.05	0.705270 ± 23	0.512614 ± 7
		Ti–Fe alkali basalt, cover	26/14b	1.70 ± 0.05	0.705230 ± 13	0.512605 ± 9
		Alkali basalt, cover	40/4	2.34 ± 0.11	0.705374 ± 10	0.512692 ± 2

Note: Nd and Sr isotopic measurements were conducted on a Finnigan 262 Mass Spectrometer at the Vinogradov Institute of Geochemistry and Analytical Chemistry, Siberian Division, Russian Academy of Sciences (G.P. Sandimirova, analyst).

separate fields representing reservoirs for alkali basaltic volcanism of the Pektusan Volcano (Fig. 1): a reservoir isotopically enriched in the Rb–Sr system (to a lesser extent, in the Sm–Nd system). The closest reservoir (in terms of isotopic characteristics) is represented by the BSE, which is considered the deepest (plume volcanism [8]) source probably located at the lower mantle–core boundary. In terms of petrogeochemical and isotopic characteristics (Tables 1, 2), the alkali high-Ti basaltoids (especially sample 26/14b) are close to the lower mantle derivatives [9]. Subalkaline basalts from the upper part of the shield volcano are plotted in the field close to the OIB sources, i.e., in the field having less radiogenic Sr but containing a DMM component. Trachybasalts in the pre-caldera vents with an age of 100–125 ka are depleted in radiogenic Sr, but enriched in radiogenic Nd as compared to other basaltoids of the volcano (0.704351 and 0.512597). This fact suggests the involvement of DMM and EM-1 components (Table 1, Fig. 1).

Data on the content of incompatible and rare earth elements (Table 2) shown in the spidergrams emphasize geochemical signatures typical of each basaltic group formed at different stages of volcanic manifestation and conditions of magma generation (Figs. 2a–2d).

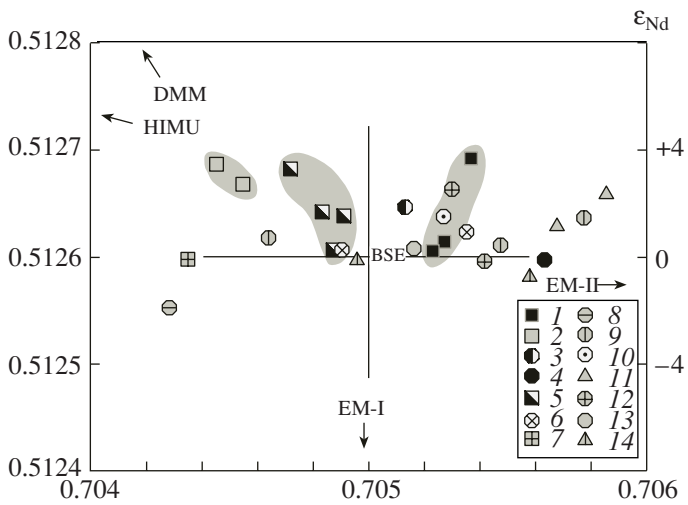

Fig. 1. Sr–Nd diagram with mantle arrays for alkali rocks of the Pektusan Volcano. Basalts and trachytes of the shield volcano: (*1*) alkali (lower) basalts, (*2*) subalkaline (upper) basalts; (*3*) trachytes. Volcanic rocks of the cone formation stage: (*4*) trachytes of the base, (*5*) alkali basalts of the vent. Caldera stage: (*6*) caldera trachyte ignimbrites (140 ka), (*7*) trachybasalt dikes (100–125 ka); (*8*) trachyte ignimbrites (95 ka), (*9*) trachyte ignimbrites and pumice (40–65 ka); (*10*) trachyte ignimbrites and ashes (~2 ka), (*11*) comendites (ashes, 969 ± 20); postcaldera stage: (*12*) trachyte ignimbrites (1702), (*13*) trachyte pumice (1903); (*14*) rhyolites and comendites (ashes, pumice, lapilli) (1903).

The differences in contents of incompatible elements between basaltoid rocks of the Pektusan Volcano and their ratios as compared to the mantle sources make it possible to reveal their nature (Table 3). Alkali basalts of the Pektusan Volcano are enriched in Rb/Sr, but depleted in the Sm/Nd and U/Pb ratios as compared to those in the primitive mantle. Such differences and comparison with alkali basalts of the Tanlu rift system [2] suggest that the isotopic ratios could be modified by host rocks or subducted sediments of the oceanic plate (Kulu). However, the $^{206}Pb/^{204}Pb$ ratios (Sakhno, in press) in some basalts do not suggest the involvement of high-Sr sediments in the magma genesis, because no correlation exists between radiogenic Sr and Pb. The Rb/Sr, Sm/Nd, and U/Pb ratios in the subalkaline basalts of the upper part of the shield volcano partly coincide with those in the primitive mantle, MORB, or OIB. Thus, the isotope data confirm the participation of different sources in the generation of basaltoid melts of shield volcanoes and vents that intrude the cone.

In the La/Nb–Ba/Nb diagram, the trend of basaltoids is close to the trend of OIB, on the one hand, and the trend of Quaternary alkali basalts of the Tan Lu rift [2], on the other hand (the former trend partially overlaps and occupies a field located above the latter trend). This is particularly typical of alkali basalts, which are plotted near data points of micaceous kimberlites. In the K/Yb–Ta/Yb diagram, the Pektusan basalt trend is shifted (relative to OIB) toward the higher K/Yb ratio owing to the lower HREE content. The high Nb–Ta/HREE ratios could be related to the low degree of partial melting of the protolith. The ratios of other incompatible elements (Table 3) confirm the above assumptions about different deep-seated sources of the basaltic melts.

Trachytes and other alkali salic rocks (pantellerites, comendites, and rhyolites), which compose the upper part of the shield volcano and Pektusan cone, represent the chamber differentiates of alkali basaltic melts. The volume of erupted trachytic melts is no more than 3 vol % of basic melts, while felsic alkali rocks (ashes and tephra) account for no more than 1 vol % of trachytes [7]. The mechanism of chamber differentiation of both basic and alkali salic melts for different cycles is confirmed by diagrams in Fig. 2.

The examination of isotope data shows that the alkali salic lavas and pyroclastic rocks (Table 1, Fig. 1) have wide variations of radiogenic Sr ratios (0.70450–0.705678), whereas $^{143}Nd/^{144}Nd$ ratios show a narrow range (0.512552–0.51262); i.e., the values of these parameters are typical of parental basaltoid melts. The higher radiogenic Sr is typical of trachytes in the upper part of the shield volcano with ages close to those of the underlying basalts (1.00 and 1.01 Ma, respectively) or to the beginning of the formation of the trachyte cone. Ashes and tephra of the explosions (for example, eruption of rhyolite ashes in 1903) have elevated $^{87}Sr/^{86}Sr$ values. However, these features are not ubiquitous. Some of these rocks, especially 95-ka-old ignimbrite explosions and others, show a high content of radiogenic Nd (Table 1).

Oxygen isotope data [7] show that $\delta^{18}O$ values are characterized by mantle signatures and are slightly decreased in the most felsic ashes of the catastrophic explosions (5.0 and 5.1 ka ago and in the years 969 and 1903) and ignimbrite explosions, i.e., in the products of gas-saturated eruptions.

One can suggest that the high content of fluids (especially H_2O, Cl, and F) is among the factors responsible for the differentiation (unmixing) of the melt and explosive eruption. Previous work [3] and our data have established that high gas contents are observed in comendites, pantellerites, and rhyolites of cycles of catastrophic eruptions of the Pektusan Volcano.

It should be noted in conclusion that the revealed heterogeneity of mantle sources in basaltoids of the Pektusan Volcano is typical of several magmatic manifestations in the Far East, for example, eruptions of basanite, leucitite, and other potassic volcanoes (Udalyanchi, Keluo, Bolon, and others) related to the East Asian superplume in the Late Mesozoic. However, the most active volcanic phase of volcanism was manifested in the Late Miocene, Late Pleistocene, and Holocene [1, 7, 9, 10, and others]. Mantle heterogeneities are typical of not only oceanic but also continental superplumes [11].

Table 2. Petrochemical composition (wt %) and contents of trace and rare earth elements (ppm) in the representative rocks of the Pektusan Volcano

Oxides	Samples											
	4	26-1a	26-1b	3a	38/4	1d	1-b	28/4b	29/3c	1i/m	26/12	28/1
SiO_2	71.72	71.09	57.82	65.73	65.87	68.05	68.07	66.41	63.89	63.18	66.85	54.86
TiO_2	0.15	0.30	0.82	0.45	0.44	0.27	0.29	0.28	0.43	0.44	0.46	2.10
Al_2O_3	10.76	10.61	17.79	14.40	14.87	14.06	14.29	11.23	15.10	17.25	15.10	16.78
Fe_2O_3	3.61	4.29	3.84	3.19	2.91	5.00	4.65	5.68	3.21	2.20	2.96	2.91
FeO	1.01	0.44	1.61	2.76	2.06	0.56	1.32	0.17	2.43	2.62	2.60	5.51
MnO	0.08	0.08	0.11	0.09	0.15	0.11	0.12	0.13	0.13	0.11	0.14	0.10
MgO	0.04	0.06	1.69	0.47	0.11	0.03	0.08	0.30	0.64	0.32	0.08	3.37
CaO	0.44	0.87	4.01	0.55	1.52	0.66	0.54	0.65	1.38	1.72	1.17	6.38
Na_2O	5.37	5.26	6.04	6.70	5.33	5.70	5.43	6.51	5.81	5.55	5.37	3.82
K_2O	4.18	3.75	4.71	5.18	5.50	4.75	4.82	4.71	6.12	5.34	4.58	2.83
P_2O_5	0.04	0.03	0.13	0.15	0.07	0.05	0.05	0.03	0.09	0.13	0.06	0.05
H_2O^-	0.22	0.44	–	0.10	–	–	0.03	–	–	–	0.16	–
L.O.I.	2.22	2.29	0.80	0.48	0.64	0.20	0.16	3.50	0.60	0.67	0.29	0.61
Total	99.82	99.51	99.43	100.25	99.53	99.89	99.85	99.59	99.83	99.53	99.82	99.49
Sc	1.09	2.38	8.36	3.37	3.74	1.92	2.39	2.57	3.71	3.94	3.92	9.45
V	1.91	3.19	36.41	3.86	0.92	1.25	3.13	1.16	1.29	7.73	0.58	87.03
Cr	87.88	38.6	59.71	125.42	30.69	88.86	129.6	23.34	27.73	92.30	25.44	95.50
Co	0.42	0.88	9.73	0.72	0.88	0.37	0.57	0.45	1.00	1.84	0.51	19.72
Ni	2.12	4.87	19.95	2.80	1.16	1.46	2.47	1.23	0.92	3.15	0.83	44.03
Ga	–	–	–	95.39	32.21	–	105.4	32.35	27.45	105.23	28.85	19.02
Ge	–	–	–	7.65	2.04	–	8.96	1.37	0.96	6.65	1.20	0.93
Rb	382.8	353.2	94.83	183.02	143.07	262.5	244.5	269.68	85.79	120.53	130.67	40.32
Sr	5.04	15.39	424.51	6.44	11.20	4.24	1.41	4.96	13.61	85.24	5.96	445.93
Y	156.0	130.53	34.07	82.11	38.01	91.86	107.7	85.59	18.37	41.14	23.66	16.56
Zr	1992.3	2470.2	562.6	1779.4	679.35	2176.8	2122.0	1881.97	630.00	670.02	872.29	347.52
Nb	239.8	301.25	71.32	175.3	75.13	220.6	224.6	261.61	96.20	74.40	129.86	41.59
Cs	6.56	5.97	1.25	2.92	1.64	3.14	3.39	5.36	1.17	1.44	0.17	0.43
Ba	10.66	14.3	1386.9	18.77	37.79	23.96	3.89	16.07	47.20	199.07	32.36	727.21
La	154.14	185.16	62.7	125.47	86.66	139.3	174.4	132.79	40.67	70.90	52.46	31.32
Ce	289.18	372.2	118.0	222.5	170.98	282.8	307.5	248.69	103.85	126.42	177.76	48.66
Pr	36.96	38.9	13.01	27.75	20.19	31.4	37.5	27.35	10.91	15.88	12.52	7.31
Nd	134.8	132.4	47.21	100.94	67.40	112.04	132.7	104.46	41.60	58.29	49.31	30.32
Sm	28.54	26.30	8.88	19.52	11.21	21.5	25.6	21.60	8.00	11.25	9.17	5.99
Eu	0.35	0.38	2.89	0.35	0.39	0.44	0.46	0.26	0.38	0.94	0.34	1.93
Gd	30.35	26.7	10.20	20.27	8.68	22.16	27.25	18.29	6.90	10.76	6.72	4.50
Tb	4.67	3.45	1.10	2.89	1.47	3.12	3.83	3.20	1.24	1.45	1.08	0.68
Dy	23.17	22.31	6.31	14.85	7.27	15.5	19.32	17.90	5.64	7.11	5.57	3.13
Ho	4.35	4.78	1.25	2.64	1.46	2.76	3.40	3.74	1.06	1.20	1.12	0.74
Er	13.36	12.86	3.15	8.27	3.59	8.58	10.83	9.06	2.70	3.67	2.77	1.32
Tm	2.12	1.88	0.44	1.34	0.54	1.41	1.72	1.41	0.39	0.59	0.48	0.24
Yb	11.51	11.76	2.98	7.16	3.42	7.64	9.32	7.97	2.40	3.24	2.79	0.94
Lu	1.54	1.77	0.43	0.95	0.56	1.08	1.33	1.14	0.39	0.46	0.53	0.18
Hf	38.2	45.82	10.23	31.63	10.67	40.5	41.84	46.50	16.01	12.44	22.33	6.01
Ta	–	17.15	4.77	7.91	2.71	9.03	9.61	14.22	4.64	–	6.49	2.04
W	–	9.38	2.16	5.71	2.25	–	–	6.46	1.90	–	1.88	0.97
Tl	–	0.60	1.62	0.50	0.18	–	–	0.62	0.21	12.44	0.18	0.07
Pb	42.14	39.16	11.3	23.71	8.99	14.50	33.63	35.91	9.88	12.47	18.27	5.61
Th	59.79	71.07	16.52	22.68	15.35	36.95	39.67	99.71	29.15	14.29	40.49	11.43
U	11.32	13.07	2.71	4.22	2.73	3.74	6.03	8.83	2.33	2.60	2.23	0.81

Table 2. (Contd.)

Oxides	Samples											
	20	38/3	21/1	28/19a	40/3	30	14/1	32	23/2	27/7	26/14b	40/4
SiO_2	64.72	69.25	50.83	51.27	49.50	67.24	64.72	51.91	53.46	46.74	46.62	46.77
TiO_2	0.44	0.25	2.92	1.72	3.45	0.39	0.44	1.79	1.69	2.69	4.45	3.06
Al_2O_3	16.60	14.73	16.96	16.05	16.11	13.81	16.60	14.25	14.97	16.27	13.09	14.78
Fe_2O_3	3.47	2.72	2.65	3.37	4.43	4.40	3.47	3.64	1.67	10.51	13.56	7.23
FeO	1.24	1.06	7.22	7.40	5.94	2.77	1.24	7.70	8.29	3.43	4.05	5.58
MnO	0.09	0.08	0.13	0.18	0.18	0.08	0.09	0.13	0.17	0.17	0.18	0.21
MgO	0.35	0.03	4.86	7.05	5.28	0.24	0.36	7.27	7.21	5.20	5.40	4.51
CaO	1.66	0.69	8.29	8.22	8.63	0.52	1.66	7.81	7.72	6.08	7.21	6.96
Na_2O	5.31	5.33	3.27	3.08	3.57	5.65	5.31	3.33	2.91	4.02	2.75	3.71
K_2O	5.35	5.25	2.34	0.93	1.96	4.51	5.35	0.93	0.85	2.96	1.83	2.18
P_2O_5	0.08	0.02	0.58	0.28	0.66	0.05	0.08	0.26	0.25	0.65	0.63	0.64
H_2O^-	0.18	–	–	–	–	–	0.18	0.25	0.58	–	0.14	0.48
L.O.I.	0.11	0.19	–	0.30	0.03	0.38	0.11	0.87	–	1.20	0.49	3.80
Total	99.60	99.59	100.06	99.85	99.74	100.07	99.60	99.85	99.77	99.87	100.06	99.91
Sc	5.99	1.52	19.40	23.53	20.28	3.14	5.99	23.25	18.42	24.45	–	16.84
V	4.29	0.98	206.62	175.57	239.62	3.64	4.29	177.8	186.9	287.5	660.1	228.74
Cr	82.50	2.77	179.30	233.11	96.36	46.76	82.50	263.8	341.3	60.53	50.55	33.87
Co	1.77	0.40	32.50	46.94	34.17	1.35	1.77	44.0	39.0	49.6	123.81	39.41
Ni	2.12	2.50	40.30	151.36	35.85	8.05	2.12	211.5	183.5	40.80	141.12	29.54
Ga	287.5	38.55	135.90	–	20.49	–	287.5	–	–	–	–	21.52
Ge	5.96	2.31	4.02	–	1.41	–	5.96	–	–	–	–	1.54
Rb	93.6	212.49	74.80	10.40	35.11	229.74	93.6	13.68	12.35	58.86	151.8	45.36
Sr	312.4	2.86	424.10	510.49	674.91	7.38	312.4	342.9	378.5	783.5	1391.9	586.68
Y	38.30	56.52	23.10	17.50	19.55	87.82	38.30	18.44	20.3	36.52	61.41	25.82
Zr	633.15	1289.75	431.50	107.76	221.47	1656.3	633.15	120.1	111.3	387.0	195.55	255.75
Nb	78.39	162.51	45.90	12.02	34.72	214.34	78.39	14.65	10.8	64.15	54.62	39.70
Cs	0.60	2.50	0.35	0.17	0.07	0.68	0.60	0.20	0.36	0.40	–	0.17
Ba	1604.9	9.65	650.90	210.4	615.82	10	1604.9	234.2	257.7	869.2	3370.9	659.25
La	68.1	115.59	38.63	11.22	33.49	170.51	68.10	12.44	11.62	58.72	59.31	40.38
Ce	132.9	212.43	72.52	23.15	70.92	331.7	132.9	25.1	22.4	122.5	149.2	86.15
Pr	16.47	27.23	9.79	3.16	9.22	33.54	16.47	3.45	3.70	13.99	19.59	10.86
Nd	61.72	86.12	39.70	13.78	34.54	112.6	61.72	14.70	16.80	52.40	98.0	40.30
Sm	10.27	15.60	8.67	4.12	6.90	19.94	10.27	4.27	5.77	10.94	22.05	7.74
Eu	3.64	0.26	3.11	1.73	2.50	0.40	3.64	1.64	1.77	3.63	7.16	2.53
Gd	10.37	11.53	8.87	2.86	6.27	24.13	10.37	2.99	5.77	11.85	20.95	6.46
Tb	1.41	1.72	1.17	0.62	0.84	2.27	1.41	0.68	0.88	1.31	2.83	1.01
Dy	6.37	10.12	5.23	3.67	4.08	14.68	6.37	3.92	4.38	7.30	15.49	5.17
Ho	1.11	2.10	0.91	0.73	0.77	3.05	1.11	0.90	0.78	1.46	2.79	1.00
Er	3.42	5.44	2.34	1.71	1.71	8.05	3.42	1.90	2.29	3.61	6.86	2.36
Tm	0.59	0.84	0.35	0.23	0.23	1.16	0.59	0.25	0.38	0.51	0.85	0.35
Yb	3.12	4.78	1.85	1.52	1.40	7.58	3.12	1.77	1.86	3.76	4.52	2.09
Lu	0.45	0.73	0.23	0.22	0.23	1.14	0.45	0.25	0.28	0.53	0.60	0.35
Hf	11.15	20.96	6.34	2.37	3.76	29.10	11.15	2.57	2.91	7.05	2.62	4.10
Ta	–	6.21	–	1.36	1.44	11.59	3.40	1.36	–	3.63	3.95	1.64
W	–	6.76	–	1.37	0.62	0.93	–	0.69	–	1.79	37.31	1.01
Tl	–	0.37	–	0.04	0.03	0.29	–	0.03	–	0.38	15.7	0.03
Pb	–	17.76	14.50	1.99	3.32	28.64	11.78	1.92	18.2	6.97	17.38	4.06
Th	–	27.57	4.34	2.08	3.81	40.5	8.40	2.56	1.53	9.20	4.53	5.11
U	–	5.50	0.73	0.29	0.38	7.58	2.06	0.40	0.23	1.60	0.83	1.01

Note: Major elements were determined at the Far East Geological Institute, Far East Division, Russian Academy of Sciences (L.I. Alekseeva, analyst). Trace elements were analyzed by ICP-MS at the Vinogradov Institute of Geochemistry and Analytical Chemistry, Siberian Division, Russian Academy of Sciences (G.P. Sandimirova and E.V. Smirnova, analysts). Sample numbers correspond to those in Table 1. Dashes denote the absence of data.

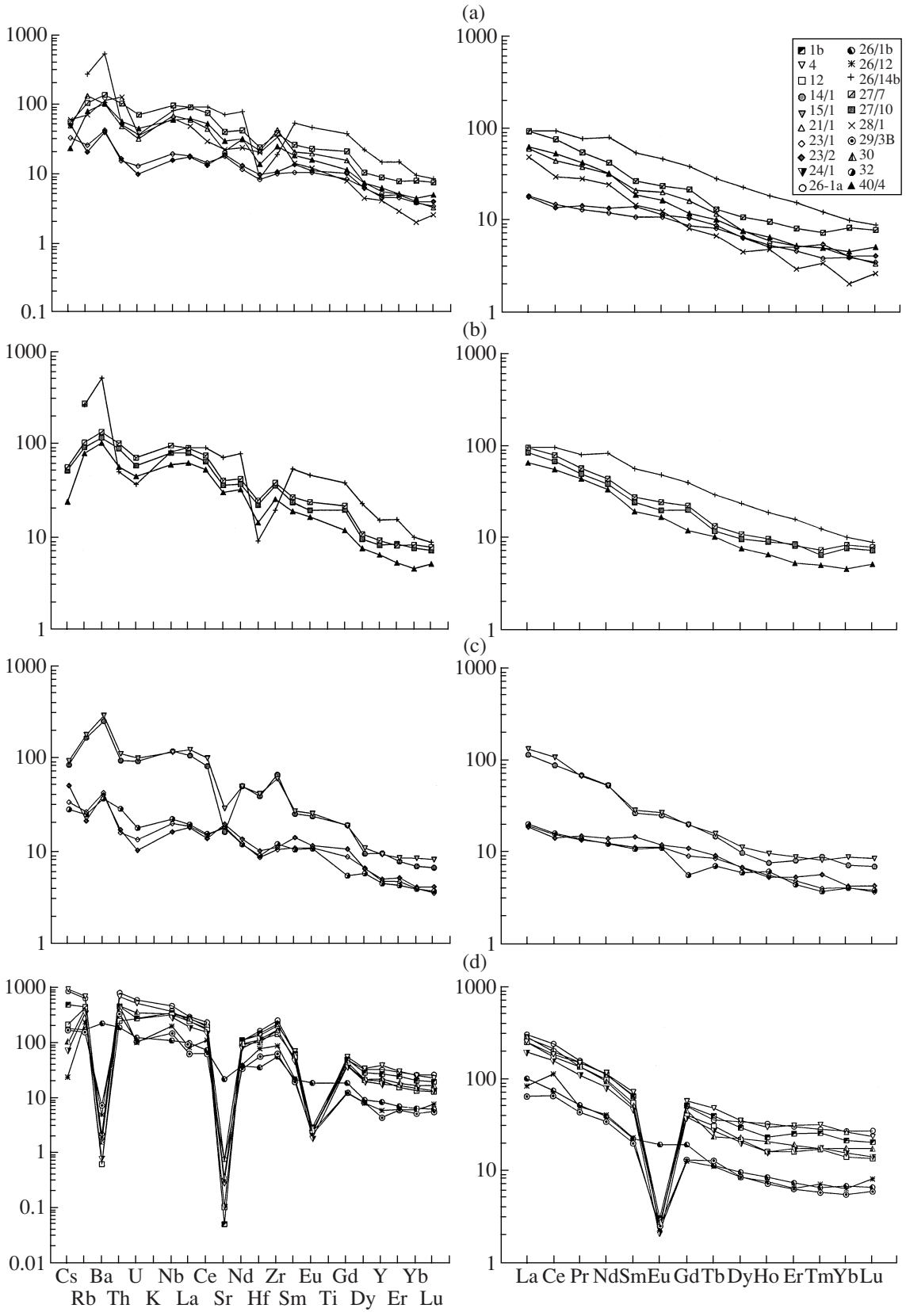

Fig. 2. Spidergrams of PM [12]-normalized trace elements. Sample numbers are as in Table 2. (a) Basalts of the Pektusan Volcano, (b) alkali basalts of the shield volcano (lower complex); (c) subalkaline basalts and trachytes of the shield volcano (upper complex); (d) alkali salic rocks (ignimbrites, pumice, ashes, and others) of the cone formation and caldera and postcaldera eruption stages.

Table 3. Ratio of incompatible elements in basaltoids of the Pektusan Volcano and mantle reservoirs

M_1/M_2	Sample													
	40/4	26/14b	27/7	7/10	32	23/1	23/2	40/3	21/1	28/19a	28/1	PM	MORB	OIB
Rb/Sr	0.08	0.11	0.08	0.07	0.04	0.04	0.03	0.05	0.18	0.02	0.09	0.030	0.006	0.047
Sm/Nd	0.20	0.22	0.21	0.21	0.29	0.30	0.34	0.20	0.22	0.30	0.20	0.325	0.360	0.260
U/Pb	0.25	0.05	0.23	0.23	0.21	0.08	0.01	0.11	0.05	0.15	0.14	0.296	0.157	0.319
Th/U	5.06	5.46	5.75	6.13	6.40	4.47	6.65	10.03	5.94	7.17	14.11	4.0	2.6	3.9
Nb/Y	1.54	0.89	1.76	1.60	0.79	0.13	0.53	1.78	1.99	0.09	2.51	0.16	0.83	1.7
Ta/Yb	0.78	0.87	0.97	0.90	0.77	0.44	–	1.03	–	0.89	2.17	0.083	0.043	1.3
Ba/Nb	16.61	61.72	13.55	14.07	15.99	18.47	23.86	17.74	14.18	17.50	17.49	98	2.7	7.3
La/Nb	1.02	1.09	0.92	0.97	0.85	0.90	1.08	0.96	0.84	0.93	0.75	0.97	1.07	0.77
Ba/La	16.33	56.84	14.80	14.54	18.83	22.81	22.18	18.39	16.84	18.75	23.22	10.1	2.5	9.5
Ba/Th	129.01	744.13	94.48	93.59	91.48	190.28	168.43	161.63	149.98	101.15	63.62	82.0	53.0	88.0
Rb/La	1.12	2.60	1.00	1.00	1.10	1.22	1.06	1.05	1.94	0.93	1.28	0.91	0.22	0.84
Ce/Pb	0.38	–	–	–	13.07	6.39	1.23	0.42	5.00	11.63	8.67	25.4	25.0	25.0
$(La/Yb)_n$	14.87	5.10	12.60	13.49	10.51	9.91	9.34	15.09	31.23	11.04	4.83	1.0	0.55	11.6

ACKNOWLEDGMENTS

This work was supported by the Presidium of the Russian Academy of Sciences (program no. 16) and the Far East Division of the Russian Academy of Sciences (project nos. 06-1-P16-065 and 06-05-9611, and contract no. 3P16-2007).

REFERENCES

1. V. G. Sakhno, *Late Mesozoic–Cenozoic Continental Volcanism of Eastern Asia* (Dal'nauka, Vladivostok, 2001) [in Russian].
2. M. Zhang, P. Suddaby, R. N. Thompson, et al., J. Petrol. **36**, 1275 (1995).
3. S. Horn and H. U. Schmincke, Bull. Volcanol. **61**, 537 (2000).
4. N. G. Razjigaeva, Volcanol. Sci. **10**, 659 (1990).
5. *Geology of Korea*, Ed. by R. J. Paek et al. (Pyongyang, 1993).
6. H. Wei, R. S. J. Sparks, R. Lu, et al., J. Asian Earth Sci. **21**, 515 (2003).
7. V. G. Sakhno, Dokl. Earth Sci. **412**, 226 (2007) [Dokl. Akad. Nauk **412**, 226 (2007)].
8. A. W. Hofmann, Nature **385**, 219 (1997).
9. A. F. Grachev, Fiz. Zemli, No. 4, 3 (2000).
10. V. V. Yarmolyuk, V. I. Kovalenko, and M. I. Kuz'min, Geotectonics, **34**, 343 (2000) [Geotektonika No. 5, 3 (2000)].
11. L. N. Kogarko, V. A. Lebedev, and L. K. Levsky, Dokl. Earth. Sci. **412**, 85 (2007) [Dokl. Akad. Nauk **412**, 240 (2007)].
12. D. A. Wood, J. Geol., No. 3, 499 (1979).